A Finite Element Analysis of a Ti:LiNbO$_3$ Traveling-Wave Electrooptic Modulator with Floating Electrodes

Marcos A. R. Franco, Angelo Passaro, Nancy M. Abe, José M. Machado* and Francisco Sircilli

Instituto de Estudos Avançados – Centro Técnico Aeroespacial – São José dos Campos – SP
* IBILCE – UNESP – São José do Rio Preto - SP

Abstract **— This work presents a quasi-static analysis of an *x*-cut Mach-Zehnder-like modulator which includes a set of floating electrodes. The results are compared to the ones obtained for a modulator of conventional electrode configuration. The electrooptic modulators were analyzed by using the finite element method. The numerical results complement information presented previously in literature.**

Index terms **— integrated optics, optical waveguides, coplanar waveguides, electrooptic modulation, finite element methods.**

I. INTRODUCTION

Electrooptic modulators with traveling-wave (TW) electrodes are one of the most important wideband devices for optical communication systems, high precision sensors, optical signal processing and optical computing. The development of technologies for the design and construction of wideband and lower power consumption modulators has demanded great efforts in the last years [1]-[8]. Particularly, our research group is engaged in the development of software systems for the analysis and design optimization of integrated optic devices and components. The analyses comprehend the influence of constructive parameters, such as, time and temperature of the ion diffusion process, different geometric configurations and materials. Results presented in literature are used regularly for the evaluation of both the adequacy of the models we adopt and the software solutions we develop.

In this work, an *x*-cut Mach-Zehnder modulator with TW electrodes and a set of extra floating electrodes is analyzed. The inclusion of the floating electrodes was proposed in [1] for an *x*-cut LiNbO$_3$ substrate, in order to increase the microwave field in the electrooptic interaction region. These floating electrodes are located between the LiNbO$_3$ substrate and the buffer layer, Fig. 1.

Both the microwave electric field and the optic field were computed in this work by applying the Finite Element Method (FEM).

The effects of the geometric parameters *G*, *g'* and *b* (Fig. 1) on the modulator performance are analyzed in order to improve the design. The results are compared to the ones obtained for a conventional *x*-cut Mach-Zehnder modulator with the same geometric characteristics.

II. THE MODEL

The Mach-Zehnder modulator manufactured with coplanar waveguides (CPW) transmission lines can be characterized by the following electrical parameters: the characteristic impedance Z_c, the effective index N_{eff} of the transverse electromagnetic (TEM) mode, the bandwidth Δf, the overlap integral factor Γ of each optical waveguide, the half-wave voltage V_π and the microwave driving power P_{in}. These parameters are defined as follows [3]-[5], [9]:

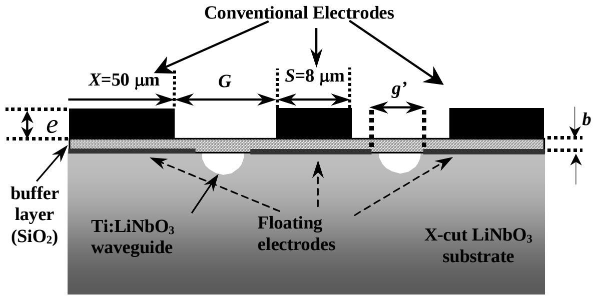

Fig. 1. *Cross-section view of the x-cut Mach-Zehnder optical modulator with a set of extra floating electrodes.*

$$Z_c = \frac{1}{c}\frac{1}{\sqrt{CC_1}}, \tag{1}$$

$$N_{eff} = \sqrt{\varepsilon_{eff}} = \sqrt{\frac{C}{C_1}}, \tag{2}$$

$$\Delta f\ L = \frac{1.4\,c}{\pi\left|\sqrt{\varepsilon_{eff}} - n_{eff}\right|} \tag{3}$$

$$\Gamma = \frac{G}{V}\frac{\iint E_{op}^2(x,y)E_{el}(x,y)\,dxdy}{\iint E_{op}^2(x,y)\,dxdy} \tag{4}$$

$$V_\pi\ L = \frac{\lambda_0\ G}{n_{be}^3\ r_{33}\left(|\Gamma_1| + |\Gamma_2|\right)} \tag{5}$$

$$P_{in} = \frac{V_\pi^2}{8Z_s\left[1-((Z_s-Z_c)/(Z_s+Z_c))^2\right]}. \tag{6}$$

In (1)-(6), C is the capacitance per unit length of the CPW with the usual materials, C_1 is the capacitance per unit length of the CPW in vacuum, c is the free-space light velocity, n_{eff} is the effective index of the optical wave, V is the static voltage between the electrodes, E_{op} is the optical electric field, E_{el} is the electric field of the

TEM wave (E_x component for the *x*-cut case), L is the length of the CPW electrodes, λ_0 is the free-space optical wavelength, n_{be} is the extraordinary refractive index of the substrate at λ_0, r_{33} is the electrooptic coefficient of $LiNbO_3$ and Z_s is the impedance of the microwave source. Notice that, for *x*-cut Mach-Zehnder modulators with optical waveguides positioned in the middle of the gap G, Fig. 1, the overlap integral for both optical waveguides, $|\Gamma_1|$ and $|\Gamma_2|$, are identical, i.e. $|\Gamma| = |\Gamma_1| = |\Gamma_2|$.

In this work, E_{el} is computed by the FEM in the quasi-static approximation (TEM modes), as follows.

The TEM modes are related to the solutions of the Laplace equation for the electric potential ϕ:

$$\nabla \cdot (\bar{\varepsilon}_r \nabla \phi) = 0, \qquad (7)$$

where the diagonal relative permittivity tensor is given by:

$$\bar{\varepsilon}_r = \begin{bmatrix} \varepsilon_{xx} & 0 \\ 0 & \varepsilon_{yy} \end{bmatrix}. \qquad (8)$$

The FEM applied to (7) yields the matrix equation:

$$[S]\,\{\phi\}^T = \{0\}^T \ , \qquad (9)$$

where :

$$[S] = \int_\Omega \left(\varepsilon_{xx} \{N\}_x^T \{N\}_x + \varepsilon_{yy} \{N\}_y^T \{N\}_y \right) dx\, dy \ , \qquad (10)$$

$$\phi = \{N\}\{\phi\}^T \text{, and } \vec{E} = -\nabla \phi \ ,$$

{ } represents a row matrix, $\{\ \}^T$ stands for a transposed matrix and $\{N\}$ represents a complete set of base functions for the used finite elements. $\{N\}_x$ and $\{N\}_y$ represent the partial derivative of the base functions in x and y coordinates.

The capacitances C and C_1 can be easily obtained from the microwave electric field. The simulations were performed for a guide built in an *x*-cut, *y*-propagating $LiNbO_3$ substrate, an isotropic buffer layer of SiO_2 and wavelength of 1.523 μm. The following parameters were assumed for the diffusion process, which determines the characteristics of the optical waveguide: initial width of Ti-strip W = 5 μm, initial thickness of Ti-strip H = 80 nm, diffusion temperature T = 1050°C and diffusion time t = 3 h [6], [10]-[12]. These parameters were chosen to guarantee the complete diffusion of Ti into the $LiNbO_3$ substrate and to produce a small optical spot size, in order to locate the optical waveguide where the electrooptic interaction is more intense.

The refractive indexes dispersion of the SiO_2 and of the $LiNbO_3$ was taken into account by using the three-terms Sellmeier equation for SiO_2 and the equivalent relations for $LiNbO_3$ presented in [8]. The electric optic field E_{op} is computed as presented in [6].

III. Results

Two modulator configurations, named conventional and floating from this time on, are considered. In the conventional configuration, three symmetrical electrodes are deposited on a plane structure composed of a SiO_2 buffer layer on a $LiNbO_3$ substrate. The floating configuration includes three floating electrodes between the substrate and the buffer layer.

The geometric parameters used for the simulations presented in this work are: electrode width X = 50 μm, central electrode width S = 8 μm, electrode thickness e = 4 μm and gap between floating electrodes g' = 5 μm (for the floating configuration only). Very thin floating electrodes (zero thickness) were assumed.

The ratio R of the modulation electric field strength E_x for the floating configuration to the conventional one:

$$R(x, y) = \frac{E_x^{float}(x, y)}{E_x^{conv}(x, y)} \ , \qquad (11)$$

and the contour lines, projected in the x-y plane, of the fundamental optical field strength in steps of 10% of the maximum optical electric field E_{op}, are shown in Fig. 2.

The ratio R and the optic-field normalized strength E_x along a vertical line which passes through the center of the optic-guide are presented in Fig. 3. Figs. 2 and 3 show clearly that the inclusion of floating electrodes results a remarkable increase of the modulator field strength in the region of maximum optic field. Thus, they increase the electrooptic interaction and reduce the power required for the operation of the modulator device, as pointed in [1].

Figs. 4 and 5 present the effective index (TEM wave) and the characteristic impedance of the conventional and floating configurations, respectively, as a function of the distance between the electrodes G and the buffer layer thickness b.

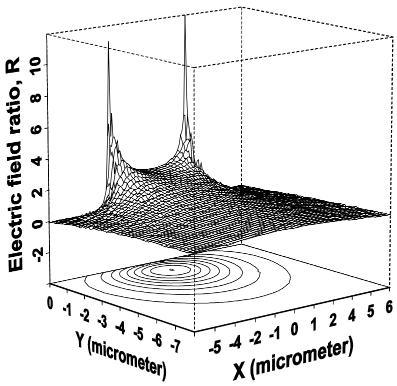

Fig. 2. *The ratio R of the modulation electric field strength E_x for the floating configuration to the conventional one. The contour lines on the x-y plane show the optic mode field distribution for the region of one of the optic guides.*

Fig. 6 presents the bandwidth variation as a function of G, for both conventional and floating configurations. The floating configuration modulator presents a greater bandwidth when compared with the conventional configuration for all gap dimensions. Fig. 7 presents the overlap integral factor Γ, and the half-wave voltage V_π as functions of the spacing dimension between floating electrodes g'. The increase of g' leads to a situation equivalent to that of a conventional layout, in other words, Γ becomes smaller and V_π grows up.

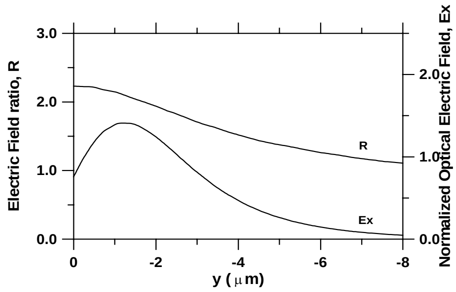

Fig. 3. *The ratio R of the modulation electric field strength E_x for the floating configuration to the conventional one and the normalized field strength for the fundamental optic mode along a vertical line which passes through the center of the gap.*

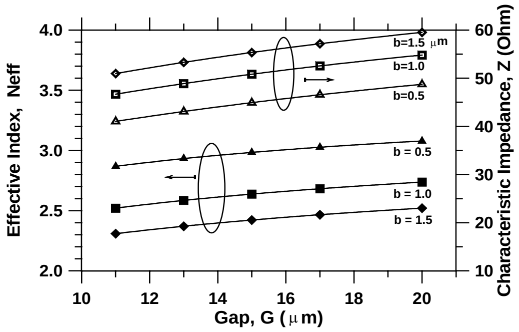

Fig. 4. *The variations of the characteristic impedance and of the effective index for a conventional configuration as a function of the distance between electrodes (gap) for various buffer layer thicknesses.*

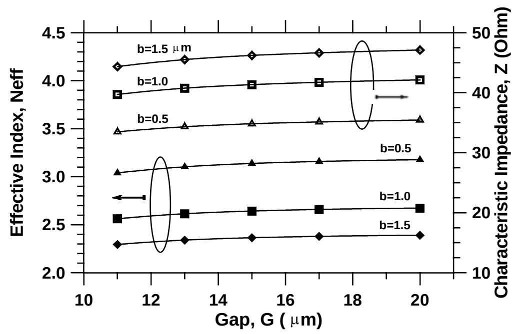

Fig. 5. *The variations of the characteristic impedance and of the effective index for a floating configuration as a function of the distance between electrodes (gap) for various buffer layer thicknesses.*

The electrical parameters of the conventional (A) and of the floating (B) configurations at the optimum electrical condition are compared in Table I. The geometrical parameters are: G = 15 μm and b = 1.5 μm. In both cases, the same Ti diffusion conditions are used. The numerical results show that the floating electrodes improve the performance of the device. A good impedance matching and larger bandwidth, 50% reduction in the half-wave voltage and a decrease of 75% in the driving power are obtained, when compared with the conventional configuration.

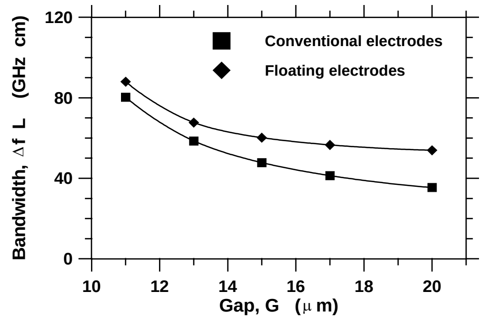

Fig. 6 *Bandwidth (Δf L) as a function of the distance between electrodes, G, for both conventional and floating configurations.*

TABLE I

ELECTRICAL PARAMETERS AT OPTIMIZED CONDITION. (A) CONVENTIONAL CONFIGURATION AND (B) FLOATING CONFIGURATION

CP W	Z (Ω)	N_{eff}	$\Delta f\ L$ (GHz cm)	$\lvert\Gamma\rvert$	$V_\pi L$ (V cm)	$P_{in} L^2$ (W cm^2)
A	55.33	2.422	47.76	0.230	16.446	0.678
B	46.20	2.364	60.16	0.463	8.193	0.168

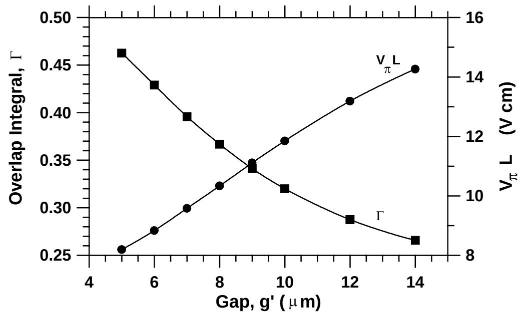

Fig. 7. *The overlap integral factor and the half-wave voltage as functions of the gap dimension g' between the floating electrodes.*

CONCLUSIONS

A *x*-cut Ti:$LiNbO_3$ traveling-wave optical modulator with extra floating electrodes was analyzed by applying the finite element method. The floating configuration allows the reduction of the effective index, the increase of the bandwidth, and the reduction of power consumption with respect to the conventional configuration. The numerical results complement information presented previously in literature. They allow the evaluation of relevant physical parameters of the optical modulators in terms of geometric dimensions of the CPW transmission lines.

REFERENCES

[1] S. Hopfer, Y. Shani and D. Nir, "A Novel, Wideband, Lithium Niobate Electrooptic Modulator," *IEEE J. Lightwave Technol.*, vol. 16, No. 1, pp. 73-77, 1998.

[2] K. Kawano, "High-Speed Shielded Velocity-Matched Ti:$LiNbO_3$ Optical Modulator," *IEEE J. Quantum Electron.*, vol. 29, No.9, pp. 2466-2475, 1993.

[3] X. Zhang and T. Miyoshi, "Optimum Design of Coplanar Waveguide for $LiNbO_3$ Optical Modulator,"

IEEE Trans. Microwave Theory Tech., vol. 43, No.3, pp. 523-528, 1995.

[4] H. Chung, W. S. C. Chang, and E. L. Adler, "Modeling and Optimization of Traveling-Wave $LiNbO_3$ Interferometric Modulators," *IEEE J. Quantum Electron.*, vol.27, No. 3, pp. 608-617, 1991.

[5] K. W. Hui, K. S. Chiang, B. Wu, and Z. H. Zhang, "Electrode Optimization for High-Speed Traveling-Wave Integrated Optic Modulators," *J. Lightwave Technol.*, vol. 16, No.2, pp.232-238, 1998.

[6] M. A. R. Franco, A. Passaro, J. R. Cardoso, and J. M. Machado, "Finite Element Analysis of Anisotropic Optical Waveguide with Arbitrary Index Profile," *IEEE Trans. Magn.*, vol.35, No.3, pp. 1546-1549, 1999.

[7] M. A. R. Franco, A. Passaro, F. Sircilli Neto, J. R. Cardoso, and J. M. Machado, "Modal Analysis of Anisotropic Diffused-Channel Waveguide by a Scalar Finite Element Method," *IEEE Trans. Magn.*, vol. 34, No. 5, pp.2783-2786, 1998.

[8] M. Koshiba, *Optical Waveguide Theory by the Finite Element Method*, 1st ed., KTK Scientific Publishers, Tokyo, 1992, pp. 126, 219-220.

[9] H. Nishihara, M. Haruna, and T. Suhara, *Optical Integrated Circuits*, 1st ed., McGraw-Hill, 1989, pp.109-111.

[10] D. Zhang, C. Chen, J. Li, G. Ding, X. Chen, and Y. Cui, "A Theoretical Study of a Ti-Diffused Er:$LiNbO_3$ Waveguide Laser," *IEEE J. Quantum Electron.*, vol. 32, N. 10, pp. 1833-1838, 1996.

[11] D. Zhang, C. Chen, G. Ding, J. Zhang, and Y. Cui, "Dependence of Ti-Diffused Er:$LiNbO_3$ Laser Efficiency on Waveguide Fabrication Parameters and Pump Wavelength," *IEEE J. Quantum Electron.*, vol. 33, No. 7, pp. 1231-1235, 1997.

[12] S. Fouchet, A. Carenco, C. Daguet, R. Guglielmi, and L. Riviere, "Wavelength Dispersion of Ti Induced Refractive Index Change in $LiNbO_3$ as a Function of Diffusion Parameters," *J. Lightwave Technol.*, vol. LT-5, N. 5, pp. 700-708, 1987.

Marcos Antonio Ruggieri Franco was graduated in Physics at Pontifícia Universidade Católica de São Paulo – Brazil (PUC-SP), in 1983. In 1991, he finished his Master of Science degree in Nuclear Physics at Instituto de Física da Universidade de São Paulo-Braxil (IFUSP). In 1999, he received his doctorate in Electrical Engineering from the Escola Politécnica da Universidade de São Paulo – Brazil (POLI-USP). In 1987, he joined the research team of the division of Applied Physics at Institute for Advanced Studies (IEAv) at Centro Técnico Aeroespacial (CTA). Since 2001, he is also associated professor of the pos-graduate course of Electronic Computation Engineering from the Instituto Tecnológico de Aeronáutica (ITA). His major areas of interest are the application of the Finite Element Method for the design of electromagnetic devices sucha as microwave and optical waveguides, fiber optics, integrated optics, antennas and electromagnetic scattering problems.
(email: marcos@ieav.cta.br)

Angelo Passaro received the B.Sc. in physics (1981) and the M.Sc degrees in nuclear physics (1988) from the Instituto de Física da Universidade de São Paulo (IFUSP), Brazil. In 1998, he completed his doctorate degree in electrical engineering at the Escola Politécnica da Universidade de São Paulo (EPUSP), Brazil. In 1984, he joined the Institute for Advanced Studies of Aerospace Technical Center. Since 1999, he has been the head of the Virtual Engineering Laboratory of (IEAv-CTA). His current research interests are in high-performance parallel programming, numerical methods, electromagnetic field computation, plasma simulation, and heat conduction analysis.
(email: angelo@ieav.cta.br)

Nancy Mieko Abe obtained the B.Sc. and M.Sc. degrees in electrical engineering from the Escola Politécnica da Universidade de São Paulo (EPUSP), Brazil, in 1989 and 1992, respectively. In 1997, she obtained the doctorate degree in electrical engineering from the same university (EPUSP). In 1998, she joined the Institute for Advanced Studies of Aerospace Technical Center (IEAv-CTA), Brazil, as a researcher fellow. Since 2002 she is an Adjunct Researcher in the Virtual Engineering Laboratory of IEAv/CTA. Her research interests include electromagnetic field computation, heat conduction analysis, plasma simulation, numerical methods and high-performance parallel programming.
(email: nancy@ieav.cta.br)

José Marcio Machado obtained his Doctorate in Electrical Engineering from the Escola Politécnica da Universidade de São Paulo (1993). In 1985, he finished his Master of Science at the Centro Brasileiro de Pesquisas Físicas (CBPF). Nowadays, he is a professor of Mathematics at the Universidade do Estado de São Paulo – Brazil (UNESP-São José do Rio Preto) at Computation Science. His major researches interests are numerical methods, differential equations and applications for Physics, Mathematics and Engineering.
(email: jmarcio@dcce.ibilce.unesp.br)

Francisco Sircilli Neto was graduated at the Institute of Physics of São Paulo University (IFUSP), Brazil, in 1981. His Master of Science was obtained in 1986 at the National Institute for Space Research (INPE), Brazil, in the area of Nuclear Geophysics. In 1997 he concluded his Doctorate in Electrical Engineering at the Polytechnic School of São Paulo University (POLI-USP), Brazil. Since 1985 he joined the research team of Division of Applied Physics of the Institute for Advanced Studies of the Aerospace Technical Center (IEAv/CTA). Today his main area of interest is the application of the Finite Element Method (FEM) to wave propagation in devices such as microwave, optical waveguides and fiber optics, as well as to antennas and electromagnetic scattering problems.
(email:sircilli@ieav.cta.br)